LETTERS
PUBLISHED ONLINE: 17 APRIL 2017 | DOI: 10.1038/NCLIMATE3274

nature climate change

The subtle origins of surface-warming hiatuses

Christopher Hedemann[1,2]*, Thorsten Mauritsen[1], Johann Jungclaus[1] and Jochem Marotzke[1]

During the first decade of the twenty-first century, the Earth's surface warmed more slowly than climate models simulated[1]. This surface-warming hiatus is attributed by some studies to model errors in external forcing[2–4], while others point to heat rearrangements in the ocean[5–10] caused by internal variability, the timing of which cannot be predicted by the models[1]. However, observational analyses disagree about which ocean region is responsible[11–16]. Here we show that the hiatus could also have been caused by internal variability in the top-of-atmosphere energy imbalance. Energy budgeting for the ocean surface layer over a 100-member historical ensemble reveals that hiatuses are caused by energy-flux deviations as small as 0.08 W m^{-2}, which can originate at the top of the atmosphere, in the ocean, or both. Budgeting with existing observations cannot constrain the origin of the recent hiatus, because the uncertainty in observations dwarfs the small flux deviations that could cause a hiatus. The sensitivity of these flux deviations to the observational dataset and to energy budget choices helps explain why previous studies conflict, and suggests that the origin of the recent hiatus may never be identified.

The surface temperature of the Earth warmed more slowly over the period 1998–2012 than could be expected by examining either most model projections or the long-term warming trend[1]. Even though some studies now attribute the deviation from the long-term trend to observational biases[17,18], the gap between observations and models persists. The observed trend deviated by as much as −0.17 °C per decade from the CMIP5 (Coupled Model Intercomparison Project Phase 5; ref. 19) ensemble-mean projection[1]—a gap two to four times the observed trend. The hiatus therefore continues to challenge climate science.

Many studies propose that heat was drawn down from the surface into deeper ocean layers by quasi-random decadal fluctuations known as internal variability. The trouble with this proposition is that most major ocean regions—the Pacific[12,14], the Indian Ocean[15], the Atlantic[10], the Atlantic and the Southern Ocean[13], and other combinations of basins[5–7,11,16]—have been named individually responsible for the heat uptake.

Here we explain these conflicting results and point to alternative interpretations. We develop a surface energy budget, which we apply to hiatuses in a 100-member historical ensemble ('the large ensemble'), generated with the coupled climate model MPI-ESM1.1 (Methods; ref. 20). Using the surface energy budget, we quantify how much deviation in energy flux occurs during a hiatus. For each hiatus in the ensemble, we then determine its origin by quantifying energy contributions to the surface from the ocean and from the top-of-atmosphere (TOA) radiative imbalance (Supplementary Fig. 1). Finally, we use the energy budget to compare interpretations of the recent hiatus in existing observations[9,21–23].

We define hiatuses in the large ensemble as any 15-year period where the GMST trend deviates by at least −0.17 °C per decade from the ensemble mean. This definition is consistent with the gap between models and observations over the period 1998–2012 (Fig. 1), as described in the Intergovernmental Panel on Climate Change Assessment Report 5 (ref. 1). Deviations in each ensemble member from the large-ensemble mean represent internal variability, which can be cleanly separated from the forced component (the ensemble mean) due to the ensemble's unprecedented size. There are hundreds of such hiatuses (364, or 2.4% of all 15,200 trends)—subject to historical forcing but due entirely to internal variability—distributed across all time periods in the ensemble (Fig. 1).

The origin of each hiatus can be deduced from energy budgeting for the ocean's surface layer (Supplementary Fig. 1), which dominates the thermal capacity of the Earth's surface and therefore mediates the decadal GMST response to flux perturbations. We consider two main flux components acting on the ocean surface layer over decadal timescales: the TOA component from above and the ocean component from below (Fig. 2a). The TOA component is the top-of-atmosphere radiative flux imbalance minus atmospheric heat uptake. The ocean component is the total heat-content change below the ocean surface layer, defined at 100 m depth. Both components are converted to ensemble anomalies (to isolate the internal variability component) from values filtered over a 15-year sliding window (see Methods) and warm the surface layer when positive.

The budget is constructed this way for two reasons. Firstly, the chosen boundary fluxes (Fig. 2a) close the surface energy budget: the sum of the TOA component and ocean component highly correlates with heat-content changes within the ocean surface layer ($r^2 = 0.97$, slope = 1.00; Supplementary Fig. 2). Other flux components (Fig. 2a) are excluded because they are small, are connected with known energy leakages, and because they do not improve budget closure (Methods and Supplementary Fig. 2). The TOA imbalance and ocean heat uptake dominate decadal internal variability in the global energy budget of other CMIP5 models as well[24]. Secondly, the ocean surface layer is defined at 100 m (as in refs 25–27), because around this depth the flux-divergence anomaly for a hiatus reaches a maximum (Fig. 2b) and is therefore the most conservative choice for our analysis. Choosing a surface depth beyond 100 m further exceeds the globally averaged mixed layer, and so the correlation between the energy budget and GMST trends sharply decays (Fig. 2b).

The energy budget allows us to determine the magnitude of flux anomalies associated with each hiatus. From the slope of the regression between surface-layer flux divergence and GMST trends, we find that the expected flux-divergence anomaly for a hiatus (a −0.17 °C per decade anomaly) is merely −0.082 W m^{-2} (Supplementary Fig. 3). This corresponds to an average cooling over the ocean's top 100 m of only −0.10 °C per decade (Methods), but the effects of that cooling are amplified at the land surface[28]. Hiatuses caused only by the ocean tend to cool the land surface more effectively, which means they generally require a lower flux-divergence anomaly than other hiatuses to achieve the same cooling.

[1]Max-Planck-Institut für Meteorologie, Bundestraße 53, 20146 Hamburg, Germany. [2]International Max Planck Research School on Earth System Modelling, Max-Planck-Institut für Meteorologie, Bundestraße 53, 20146 Hamburg, Germany. *e-mail: christopher.hedemann@mpimet.mpg.de

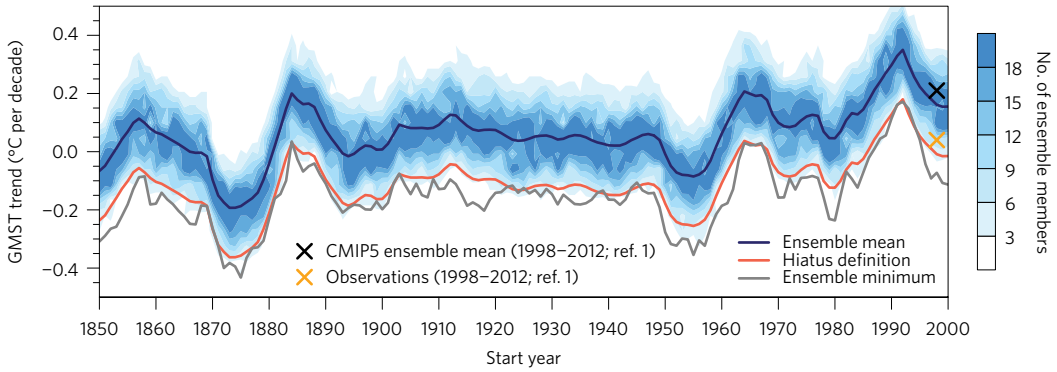

Figure 1 | Distribution of 15-year trends in global mean surface temperature (GMST) in the 100-member ensemble. The coupled climate model MPI-ESM1.1 is forced with CMIP5-prescribed historical forcing from 1850 until 2005, and extended until 2015 with the RCP4.5 scenario (see Methods). When the red line lies above the grey line, at least one ensemble member is experiencing a hiatus, defined as a deviation of more than 0.17 °C per decade below the ensemble mean. This deviation is the same as the gap between the CMIP5 ensemble mean (black cross) and the observed (yellow cross) GMST trends for the period 1998–2012. Contours represent the number of ensemble members in bins of 0.05 °C per decade.

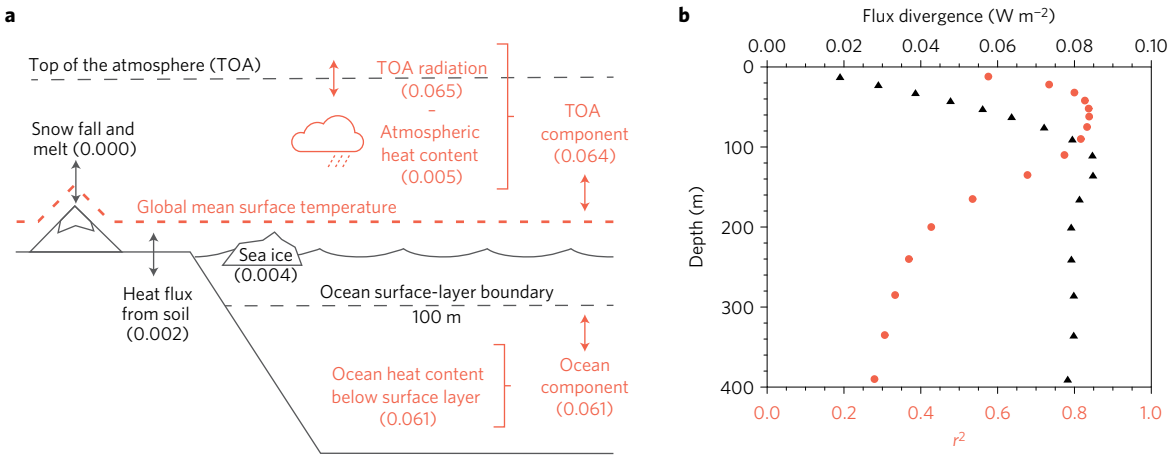

Figure 2 | Surface energy budgets. a, The surface energy budget in the large ensemble. Red colouring indicates the global mean surface temperature (GMST) and the components included in the surface-layer flux divergence. The smaller flux components in black are excluded because they do not improve budget closure or the relationship with GMST trends. Numbers in brackets represent the variability of each heat flux (W m^{-2}), given as the root mean square of 15-year ensemble anomalies. **b**, Results from surface budgets determined by increasingly deeper definitions of the ocean surface layer. For each depth, a linear regression is performed for GMST trends against the surface-layer flux divergence (both as 15-year ensemble anomalies). Shown in black (top axis) is the expected deviation in flux divergence required to cause a hiatus, calculated from the regression slope. Shown in red (bottom axis) is the correlation (r^2) of each regression. The correlation rapidly deteriorates for definitions of the surface layer below 100 m.

Variation in the ratio of land to ocean surface-cooling leads to variation around the expected flux-divergence anomaly: an interval of -0.082 ± 0.038 W m^{-2} covers the 5–95% range for all hiatuses. These results suggest that the total combined anomaly in TOA fluxes and ocean heat uptake that caused the gap between observations and models during the hiatus could be on the order of 0.1 W m^{-2}. Defining hiatuses as equal to the observed 1998–2012 anomaly from the long-term observed trend (an anomaly of 0.04–0.07 °C per decade) would reduce the threshold to just 0.02–0.03 W m^{-2}.

Across the large ensemble, the 0.082 W m^{-2} threshold in energy flux is frequently exceeded by anomalous heat-content changes in all major ocean basins, especially in the Atlantic, Pacific and Southern Ocean (Fig. 3b). However, these heat-content changes are dominated by interbasin heat exchange, which does not contribute to the surface-layer flux divergence. In each major basin, the variations in heat content below the surface layer cannot predict trends in GMST (Fig. 3a and Supplementary Fig. 4), and indeed would falsely predict many more hiatuses than actually occur.

Even the global ocean heat uptake below 100 m correlates poorly with GMST trends (Fig. 3a). The TOA component tends to oppose the ocean component's contribution to the energy budget, as demonstrated by the negative correlation in Fig. 3c. The flux-divergence anomaly, which has less than half the variability of either the TOA or ocean component alone (Fig. 3b), is the only reliable predictor of GMST trends (Fig. 3a).

The role of the TOA and the ocean in each hiatus can be determined by comparing their relative contributions to the flux-divergence anomaly. For hiatuses in the large historical ensemble, the negative (cooling) anomaly is caused entirely by the TOA in 12% of cases and by the ocean in 24% of cases. In the remainder (64%), the negative anomaly is caused by the TOA and ocean acting together (bottom left quadrant of Fig. 3c). TOA variability is therefore involved in 76% of all hiatuses.

Applying a similar analysis to observations should reveal the energetic origin of the gap between models and observations during the recent hiatus (Supplementary Fig. 1). We convert two observation-based estimates of fluxes over 2000–2010 to anomalies by subtracting the mean energy budget of the large ensemble for the same period (Methods). These anomalies include both the effect of internal variability and any potential effects of forcing differences between model and observations. Choosing 2000–2010 means that we do not cover the full hiatus period (1998–2012)

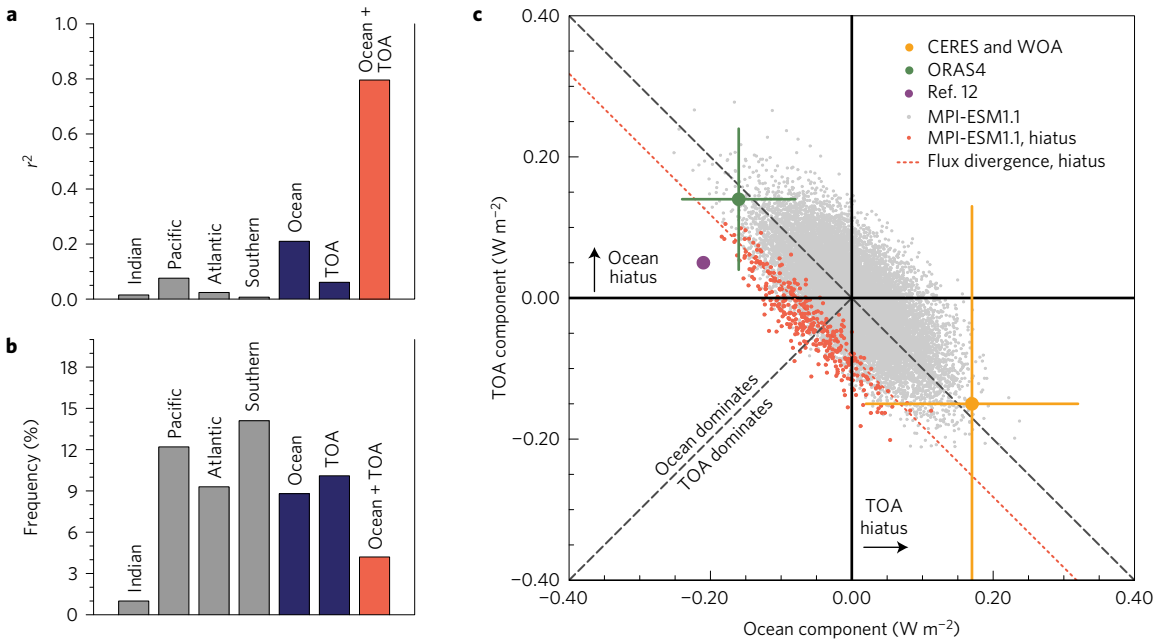

Figure 3 | Hiatuses and their origins in models and observations. a, Correlation between global mean surface temperature (GMST) trends and heat fluxes in the large ensemble (as 15-year ensemble anomalies). **b**, Frequency with which each component exceeds the expected threshold for a hiatus (−0.082 W m^{-2}). In **a** and **b**, grey bars represent changes in ocean heat content below the ocean surface layer (100 m) by basin, blue bars represent the ocean and TOA components, and the red bar is the surface-layer flux divergence (TOA + ocean components). **c**, Contributions to hiatuses from TOA and ocean components. Positive values indicate fluxes that warm the surface. Small red dots represent hiatuses in the large ensemble and small grey dots represent all other trends; the red dotted line is a flux divergence of −0.082 W m^{-2}. Observational estimates and their 1-sigma error bars are compiled from multiple sources that rely either on CERES[21] and WOA data[22] (large yellow dot) or ORAS4 data[9,23] (large green dot), shown as anomalies from the large-ensemble mean budget over the 2000s (−0.66 W m^{-2} for the ocean and +0.77 W m^{-2} for the TOA component). The large purple dot represents results from an ocean model forced with reanalysis-based winds as reported in ref. 12, converted to mean fluxes over 15 years.

and that the corresponding gap in GMST trend between models and observations is reduced, because the warming rate increased after 2000[18]. However, this choice allows us to construct temporally consistent energy budgets from multiple sources and to take advantage of the improved quality of observations after 2000. Although the budgets do not cover the full hiatus period, they do illustrate how observational uncertainty affects interpretations of the hiatus. The first budget uses WOA ocean observations[22] and a recent estimate of TOA fluxes based on the CERES satellite data product, Argo floats and AMIP simulations[21]. This first budget suggests that the hiatus was caused purely by the reduced influx of energy at the TOA (yellow dot, Fig. 3c). The second budget, based on ocean reanalysis data from ORAS4 (refs 9,23), suggests the hiatus was caused purely by increased heat uptake in the ocean (green dot, Fig. 3c). The anomalies diagnosed from an ocean model forced with the exceptional Pacific trade winds observed during the hiatus[12] likewise suggest an ocean origin (purple dot, Fig. 3c).

From our analysis of observational estimates, we are unable to exclude the TOA anomaly as a possible cause of the recent hiatus. Referencing the observations to an alternative energy budget (rather than that of the large ensemble) could shift the absolute position of the green and yellow crosses in Fig. 3c. However, their relative distance from one another and the size of their error bars would not change.

Interpretations of the hiatus are also sensitive to the energy budgeting method used, and this may reveal why the results of previous studies conflict. For example, the hiatus has been explained as the result of heat being transferred from the surface ocean to the layers immediately below it, in the upper 300–350 m (refs 14,16). However, an energy budget that accounts only for heat exchange between the top 100 m and depths up to 300–350 m correlates poorly with GMST trends in the large ensemble ($r^2 = 0.08$, Supplementary Fig. 5). A poor correlation also results when we exclude heat-content changes below the upper 700 m ($r^2 = 0.14$, Supplementary Fig. 5; see ref. 15) and the upper 2,000 m of ocean ($r^2 = 0.36$, Supplementary Fig. 5; see ref. 13). Heat-content changes up to as much as 4,000 m may be important for decadal internal variability (Supplementary Fig. 5), despite claims to the contrary[16]. Furthermore, the pattern of surface-layer cooling overlying a warming trend may be common during ocean hiatuses, but it also occurs in around half of hiatuses caused purely by the TOA (Supplementary Fig. 6). During these TOA hiatuses, the subsurface warming is caused by heat transfer from deeper layers. Energy budgets that do not consider uptake across the whole ocean depth may therefore misrepresent crucial energy fluxes and misdiagnose the hiatus.

The hiatus may also be misdiagnosed by misrepresenting the surface layer in energy budgeting. For example, the surface layer has been defined at 300 m ocean depth or more[5,6,8–10,13]. We perform energy budgeting in the large ensemble with a surface layer that extends to 300 m instead of 100 m and find that the flux-divergence correlates comparatively poorly with GMST trends ($r^2 = 0.33$ for 300 m, Fig. 2b).

We conclude that the TOA may have been a source of significant internal variability during the hiatus. Our conclusions are not an artefact of model-generated TOA variability[29]—the large ensemble produces TOA variability that is similar to that in the observational record (Supplementary Fig. 7). Rather, our conclusions are based on a simple yet robust principle, namely that the Earth's surface layer has a small heat capacity. The surface temperature can therefore be influenced by small variations in the large yet mutually compensating fluxes that make up this layer's energy budget. Comparing the small variability in the TOA imbalance with the total TOA imbalance under global warming[27,30] obscures the significance of these small variations for the hiatus.

Other observational studies associate the hiatus with heat-flux anomalies that range from 0.21 W m^{-2} (ref. 30) to 0.50 W m^{-2} (ref. 11). But when we perform energy budgeting for the surface layer in the large ensemble, we find that anomalies closer to 0.08 W m^{-2} can account for hiatuses as large as 0.17 °C per decade, and 0.02–0.03 W m^{-2} for a hiatus equal to the 1998–2012 anomaly from the observed long-term trend. Because the flux-divergence anomaly is so small, ascribing the origin of the recent hiatus to the TOA or ocean requires that each of their contributions to the anomaly are known with considerable accuracy. However, the uncertainty in TOA imbalance from satellite measurements is two orders of magnitude larger (∼8 W m^{-2}; ref. 31) than the anomaly we calculate. Satellite data are commonly anchored with ocean heat-content measurements, but the uncertainty range in TOA imbalance during the 2000s still remains around 0.56 W m^{-2} (ref. 21), and even for the most recent estimate based on improved ocean observations over 2005–2015, the range is 0.2 W m^{-2} (ref. 32).

This is the true dilemma at the heart of the hiatus debate: the variability in ocean heat content alone has no power to explain the hiatus, and the measure that can—the surface-layer flux divergence—is dwarfed by observational uncertainty. While there are attempts to fill the gaps in observations with ocean reanalyses such as ORAS4 (refs 9,23), the resulting data are of questionable integrity during the hiatus[14,21] and, as we show, disagree with the budget based on CERES[21] and WOA[22]. Even if these disagreements could be reconciled, the process of anchoring satellite observations with ocean heat uptake makes the contributions from TOA and ocean difficult to disentangle, because their absolute difference is unknown. Therefore, unless the uncertainty of observational estimates can be considerably reduced, the true origin of the recent hiatus may never be determined.

Methods

Methods, including statements of data availability and any associated accession codes and references, are available in the online version of this paper.

Received 12 July 2016; accepted 17 March 2017; published online 17 April 2017

References

1. Flato, G. *et al*. in *Climate Change 2013: The Physical Science Basis* (eds Stocker, T. F. *et al*.) 741–866 (IPCC, Cambridge Univ. Press, 2013).
2. Solomon, S. *et al*. The persistently variable 'background' stratospheric aerosol layer and global climate change. *Science* **333,** 866–870 (2011).
3. Santer, B. D. *et al*. Volcanic contribution to decadal changes in tropospheric temperature. *Nat. Geosci.* **7,** 185–189 (2014).
4. Kopp, G. & Lean, J. L. A new, lower value of total solar irradiance: evidence and climate significance. *Geophys. Res. Lett.* **38,** L01706 (2011).
5. Meehl, G. A., Arblaster, J. M., Fasullo, J. T., Hu, A. & Trenberth, K. E. Model-based evidence of deep-ocean heat uptake during surface-temperature hiatus periods. *Nat. Clim. Change* **1,** 360–364 (2011).
6. Meehl, G. A., Hu, A., Arblaster, J. M., Fasullo, J. & Trenberth, K. E. Externally forced and internally generated decadal climate variability associated with the Interdecadal Pacific Oscillation. *J. Clim.* **26,** 7298–7310 (2013).
7. Guemas, V., Doblas-Reyes, F. J., Andreu-Burillo, I. & Asif, M. Retrospective prediction of the global warming slowdown in the past decade. *Nat. Clim. Change* **3,** 649–653 (2013).
8. Watanabe, M. *et al*. Strengthening of ocean heat uptake efficiency associated with the recent climate hiatus. *Geophys. Res. Lett.* **40,** 3175–3179 (2013).
9. Balmaseda, M. A., Trenberth, K. E. & Källén, E. Distinctive climate signals in reanalysis of global ocean heat content. *Geophys. Res. Lett.* **40,** 1754–1759 (2013).
10. Katsman, C. A. & van Oldenborgh, G. J. Tracing the upper ocean's 'missing heat'. *Geophys. Res. Lett.* **38,** L14610 (2011).
11. Drijfhout, S. S. *et al*. Surface warming hiatus caused by increased heat uptake across multiple ocean basins. *Geophys. Res. Lett.* **41,** 7868–7874 (2014).
12. England, M. H. *et al*. Recent intensification of wind-driven circulation in the Pacific and the ongoing warming hiatus. *Nat. Clim. Change* **4,** 222–227 (2014).
13. Chen, X. & Tung, K.-K. Varying planetary heat sink led to global-warming slowdown and acceleration. *Science* **345,** 897–903 (2014).
14. Nieves, V., Willis, J. K. & Patzert, W. C. Recent hiatus caused by decadal shift in Indo-Pacific heating. *Science* **349,** 532–535 (2015).
15. Lee, S.-K. *et al*. Pacific origin of the abrupt increase in Indian Ocean heat content during the warming hiatus. *Nat. Geosci.* **8,** 445–449 (2015).
16. Liu, W., Xie, S.-P. & Lu, J. Tracking ocean heat uptake during the surface warming hiatus. *Nat. Commun.* **7,** 10926 (2016).
17. Cowtan, K. & Way, R. G. Coverage bias in the HadCRUT4 temperature series and its impact on recent temperature trends. *Q. J. R. Meteorol. Soc.* **140,** 1935–1944 (2014).
18. Karl, T. R. *et al*. Possible artifacts of data biases in the recent global surface warming hiatus. *Science* **348,** 1469–1472 (2015).
19. Taylor, K. E., Stouffer, R. J. & Meehl, G. A. An overview of CMIP5 and the experiment design. *Bull. Am. Meteorol. Soc.* **93,** 485–498 (2012).
20. Giorgetta, M. A. *et al*. Climate and carbon cycle changes from 1850 to 2100 in MPI-ESM simulations for the Coupled Model Intercomparison Project phase 5. *J. Adv. Model. Earth Syst.* **5,** 572–597 (2013).
21. Smith, D. M. *et al*. Earth's energy imbalance since 1960 in observations and CMIP5 models. *Geophys. Res. Lett.* **42,** 1205–1213 (2015).
22. Levitus, S. *et al*. World ocean heat content and thermosteric sea level change (0–2000 m), 1955–2010. *Geophys. Res. Lett.* **39,** L10603 (2012).
23. Trenberth, K. E., Fasullo, J. T. & Balmaseda, M. A. Earth's energy imbalance. *J. Clim.* **27,** 3129–3144 (2014).
24. Palmer, M. D. & McNeall, D. J. Internal variability of Earth's energy budget simulated by CMIP5 climate models. *Environ. Res. Lett.* **9,** 034016 (2014).
25. Baker, M. B. & Roe, G. H. The shape of things to come: why is climate change so predictable? *J. Clim.* **22,** 4574–4589 (2009).
26. Geoffroy, O. *et al*. Transient climate response in a two-layer energy-balance model. Part I: analytical solution and parameter calibration using CMIP5 AOGCM experiments. *J. Clim.* **26,** 1841–1857 (2013).
27. Brown, P. T., Li, W., Li, L. & Ming, Y. Top-of-atmosphere radiative contribution to unforced decadal global temperature variability in climate models. *Geophys. Res. Lett.* **41,** 5175–5183 (2014).
28. Byrne, P. B. & O'Gorman, P. A. Land-ocean warming contrast over a wide range of climates: convective quasi-equilibrium theory and idealized simulations. *J. Clim.* **26,** 4000–4016 (2013).
29. Stephens, G. L. *et al*. The albedo of Earth. *Rev. Geophys.* **53,** 141–163 (2015).
30. Trenberth, K. E. & Fasullo, J. T. An apparent hiatus in global warming? *Earth's Future* **1,** 19–32 (2013).
31. Loeb, N. G. *et al*. Toward optimal closure of the Earth's top-of-atmosphere radiation budget. *J. Clim.* **22,** 748–766 (2009).
32. Johnson, G. C., Lyman, J. M. & Loeb, N. G. Improving estimates of Earth's energy imbalance. *Nat. Clim. Change* **6,** 639–640 (2016).

Acknowledgements

This work is supported by the Max Planck Society for the Advancement of Science through the International Max Planck Research School on Earth System Modelling (IMPRS-ESM). J.J. acknowledges support from the European Union's Horizon 2020 research and innovation programme (grant agreement no 633211). We thank H. Haak for his technical assistance, H. Zuo and D. Peterson for providing the NEMO grid configuration, and B. Stevens and C. Li for their comments on the manuscript. We are indebted to L. Kornblueh for producing the large historical ensemble and to T. Schulthess and the Swiss National Computing Centre (CSCS) for providing the necessary computational resources. Thanks also to J. Kröger for producing the RCP4.5 extensions with the Deutsches Klimarechenzentrum (DKRZ) facilities.

Author contributions

C.H. and J.M. conceived the original idea for this study. C.H. developed the methodology and performed the analysis. All authors discussed the results. C.H. wrote the manuscript with input from J.M., T.M. and J.J.

Additional information

Supplementary information is available in the online version of the paper. Reprints and permissions information is available online at www.nature.com/reprints. Publisher's note: Springer Nature remains neutral with regard to jurisdictional claims in published maps and institutional affiliations. Correspondence and requests for materials should be addressed to C.H.

Competing financial interests

The authors declare no competing financial interests.

Methods

The large historical ensemble in this study was generated by the Max Planck Institute Earth System Model version 1.1 (MPI-ESM1.1), an incremental improvement of the coupled ocean–atmosphere general circulation model submitted to CMIP5 in the LR configuration[20], which has T63/1.9° horizontal resolution in the atmosphere and approximately 1.5° horizontal resolution in the ocean. The 100 ensemble members were generated under CMIP5 historical forcing from 1850 until 2005, with extensions to 2015 under the RCP4.5 scenario[20]. The ensemble's internal variability of 15-year GMST trends (5–95% range of 0.30 °C per decade) is slightly larger than an estimate for the CMIP5 ensemble (5–95% range of 0.26 °C per decade; ref. 33).

GMST trends are calculated from the slope of an ordinary least-squares linear regression over a 15-year sliding window, to be consistent with the hiatus as described in ref. 1. Ensemble anomalies are then calculated at each time step: $X'_{t,n} = X_{t,n} - (1/100)\sum_{n=1}^{100} X_{t,n}$, where t is the time step and n is the ensemble member.

The composition of the energy budget is chosen to maximize the correlation of the surface-layer flux divergence with both GMST trends and changes in ocean surface-layer heat content.

For the comparison with GMST trends (Supplementary Fig. 3) and most of this study, any terms expressed as heat content (joules) are converted to trend anomalies in the same way as GMST, and then converted to units of W m^{-2} over the total surface area of the Earth. All energy fluxes that are output from the model as W m^{-2} are first time-integrated and then treated the same as heat content. This step ensures the same time-filtering for all aspects of the energy budget, and thereby prevents the introduction of significant errors. In the case of the net TOA imbalance, an energy-leakage constant of 0.44 W m^{-2} is first estimated from 2,000 years of the control run and then removed. Leakage is energy destroyed by model errors; MPI-ESM1.1 has improved energy conservation compared to its predecessor, MPI-ESM, and both have relatively small leakage compared to models in the CMIP5 ensemble[34].

The comparison between flux divergence and ocean surface-layer heat content (Supplementary Fig. 2) uses a slightly different approach. To test for exact changes in heat content over a 15-year period, only the start and end states are relevant. The least-squares method is, however, influenced by the pathway from start to end states. Instead, a difference filter is calculated from the start and end years in the 15-year sliding window, divided by the time difference of 14 years: $\Delta X_t = (1/14)(X_{t+14} - X_t)$.

The selected flux divergence is the sum of two components: the TOA radiative imbalance minus atmospheric heat uptake (trends in vertically integrated moist static energy); and trends in ocean heat content below the ocean surface layer. This is the simplest flux combination that matches the expected one-to-one relationship between flux divergence and change in surface-layer heat content (Supplementary Fig. 2). The salient characteristic of the ocean surface layer for this study is the relationship between heat-content changes within the layer and resulting changes in GMST. The surface-layer depth of 100 m is therefore chosen to maintain the high correlation between the flux divergence and GMST trends (Fig. 2b), but remains a conservative choice for estimation of the flux-divergence threshold during hiatuses. Removing heat changes that are related to phase changes (land-ice and sea-ice changes) or including the heat flux from the soil does not improve the relationship with GMST trends (Supplementary Fig. 3).

The expected surface-layer flux divergence associated with a hiatus is calculated from the slope of the regression between flux divergence and GMST trends. The value we calculate (−0.082 W m^{-2}) is less than the flux divergence required by uniform cooling of −0.17 °C per decade in the top 100 m of ocean: −0.150 W m^{-2}. This is because the layer cools on average by only −0.10 °C per decade during hiatuses, which matches the theoretically expected cooling if the total anomaly of −0.082 W m^{-2} were focused in the ocean surface layer. The error interval of ±0.038 W m^{-2} is calculated from the 5–95% range of all regression residuals of flux divergence during hiatuses in the ensemble. There is no significant relationship between the origin of hiatuses and different periods in time (Supplementary Table 2).

The heat-content changes for individual basins are calculated from linear trends in heat content below 100 m. Basin boundaries are identical to those used in CMIP5 and can be downloaded from the quality-control data in ref. 35.

Observational estimates in Fig. 3c rely on a combination of data sources, which are summarized below and quantified in Supplementary Table 1. The CERES and WOA estimate for the 2000s is composed from the estimate of TOA fluxes in ref. 21, and an estimate of heat uptake using WOA data[22], including pentadal heat-content values for 700 m–2,000 m, yearly heat-content values for the upper 700 m, and a separate estimate for deep-ocean warming[36]. From the total heat uptake, we subtract the heat-content trend for the first 100 m in the WOA objective analysis data[22] (calculated from *in situ* temperature with a constant density and specific heat of 4×10^6 J m^{-3} °C^{-1}).

For this first budget, the 1-sigma error bars for the TOA estimate are taken from the same source as the estimate itself[21]. The error bars for the WOA ocean heat-content trend are calculated as plus or minus the standard error of the slope parameter, assuming that the errors in heat content are auto-correlated and behave like an AR(1) process[37,38]. The auto-correlation coefficient for the errors is estimated from residuals in heat-content data preceding the 2000s (1957–1999). A reduced degrees of freedom is calculated from the auto-correlation coefficient and scales the estimate of the standard error in heat content, which is calculated directly from the error estimates provided with the WOA data[22] (not from the regression residuals).

The ORAS4 ocean anomaly is calculated using an estimate for the total-depth heat uptake in the 2000s (ref. 9) minus the trend for the top 100 m, which is calculated from the available ORAS4 potential temperature values with a constant density and specific heat of 4×10^6 J m^{-3} °C^{-1}. The 1-sigma error bars are taken directly from ref. 9. For this second budget, the corresponding TOA flux estimate and its error bars are taken from ref. 23.

For both observation-based budgets, we remove the effect of ocean drift in the large ensemble. A quadratic function is first fitted to ocean heat content over the 2000-year control run[39]. Since each ensemble member starts from a different point in the control run, the drift is estimated from the rate of change in the quadratic that corresponds to each ensemble member's midpoint. The resulting ensemble-mean drift of 0.01 W m^{-2} is removed from both the ocean component and the TOA component.

In ref. 12, the budget is given as anomalies from the control experiment in total heat-content change for the top 125 m of ocean and the remaining ocean. We convert these values to 15-year fluxes over the total Earth surface. We assume that the anomaly below 125 m represents the ocean component, and the sum of surface and deep-ocean components is equivalent to the TOA component.

Code availability. The MPI-ESM1.1 model version was used to generate the large ensemble and is available at http://www.mpimet.mpg.de/en/science/models/mpi-esm.html. Computer code used in post-processing of raw data has been deposited with the Max Planck Society: http://pubman.mpdl.mpg.de/pubman/faces/viewItemFullPage.jsp?itemId=escidoc:2353695.

Data availability. Raw data from the large ensemble were generated at the Swiss National Computing Centre (CSCS) and Deutsches Klimarechenzentrum (DKRZ) facilities. Derived data have been deposited with the Max Planck Society (http://pubman.mpdl.mpg.de/pubman/faces/viewItemFullPage.jsp?itemId=escidoc:2353695). Supplementary Fig. 7 uses TOA flux reconstructions provided by R Allan[40] (http://www.met.reading.ac.uk/~sgs01cll/flux) and satellite observations provided by the NASA CERES project[31] (http://ceres.larc.nasa.gov). For observational estimates in Fig. 3c, we make use of data provided by the NOAA World Ocean Atlas[22] (https://www.nodc.noaa.gov/OC5/3M_HEAT_CONTENT) and by the ECMWF Ocean Reanalysis System 4 (ref. 9; http://icdc.zmaw.de/projekte/easy-init/easy-init-ocean.html).

References

33. Marotzke, J. & Forster, P. M. Forcing, feedback and internal variability in global temperature trends. *Nature* **517,** 565–570 (2015).
34. Mauritsen, T. *et al*. Tuning the climate of a global model. *J. Adv. Model. Earth Syst.* **4,** M00A01 (2012).
35. Jungclaus, J. *et al*. *CMIP5 Simulations of the Max Planck Institute for Meteorology (MPI-M) Based on the MPI-ESM-LR model: The Decadal2000 Experiment, Served by ESGF* (World Data Center for Climate at DKRZ, 2013); http://dx.doi.org/10.1594/WDCC/CMIP5.MXEL00
36. Purkey, S. G. & Johnson, G. C. Warming of global abyssal and deep Southern Ocean waters between the 1990s and 2000s: contributions to global heat and sea level rise budgets. *J. Clim.* **23,** 6336–6351 (2010).
37. Hartmann, D. L. *et al*. in *Climate Change 2013: The Physical Science Basis* (eds Stocker, T. F. *et al*.) 2SM-1–2SM-30 (IPCC, Cambridge Univ. Press, 2013).
38. Santer, B. D. *et al*. Consistency of modelled and observed temperature trends in the tropical troposphere. *Int. J. Climatol.* **28,** 1703–1722 (2008).
39. Sen Gupta, A., Jourdain, N. C., Brown, J. N. & Monselesan, D. Climate drift in the CMIP5 models. *J. Clim.* **26,** 8597–8615 (2013).
40. Allan, R. P. *et al*. Changes in global net radiative imbalance 1985–2012. *Geophys. Res. Lett.* **41,** 5588–5598 (2014).